

University of Groningen

Optical dephasing in solution

Nibbering, Erik T. J.; Duppen, Koos; Wiersma, Douwe A.

Published in:
The Journal of Chemical Physics

DOI:
[10.1063/1.459617](https://doi.org/10.1063/1.459617)

IMPORTANT NOTE: You are advised to consult the publisher's version (publisher's PDF) if you wish to cite from it. Please check the document version below.

Document Version
Publisher's PDF, also known as Version of record

Publication date:
1990

[Link to publication in University of Groningen/UMCG research database](#)

Citation for published version (APA):

Nibbering, E. T. J., Duppen, K., & Wiersma, D. A. (1990). Optical dephasing in solution: a line shape and resonance light scattering study of azulene in isopentane and cyclohexane. *The Journal of Chemical Physics*, 93(8), 5477-5484. <https://doi.org/10.1063/1.459617>

Copyright

Other than for strictly personal use, it is not permitted to download or to forward/distribute the text or part of it without the consent of the author(s) and/or copyright holder(s), unless the work is under an open content license (like Creative Commons).

The publication may also be distributed here under the terms of Article 25fa of the Dutch Copyright Act, indicated by the "Taverne" license. More information can be found on the University of Groningen website: <https://www.rug.nl/library/open-access/self-archiving-pure/taverne-amendment>.

Take-down policy

If you believe that this document breaches copyright please contact us providing details, and we will remove access to the work immediately and investigate your claim.

Downloaded from the University of Groningen/UMCG research database (Pure): <http://www.rug.nl/research/portal>. For technical reasons the number of authors shown on this cover page is limited to 10 maximum.

Optical dephasing in solution: A line shape and resonance light scattering study of azulene in isopentane and cyclohexane

Erik T. J. Nibbering, Koos Duppen, and Douwe A. Wiersma

Department of Chemistry, Ultrafast Laser and Spectroscopy Laboratory, University of Groningen, Nijenborgh 16, 9747 AG, Groningen, The Netherlands

(Received 26 December 1989; accepted 2 July 1990)

Results of a line shape and resonance light scattering study of the $S_1 \leftarrow S_0$ and $S_2 \leftarrow S_0$ electronic transitions of azulene in isopentane and cyclohexane are reported. The results are analyzed using two different non-Markovian master equations that make different assumptions about the statistical properties of the bath. For both these origin transitions we find that the solution dynamics fall in the so-called intermediate modulation regime. If exponential decay is assumed for the bath correlation function we obtain a correlation time of the bath of 25 fs for the $S_1 \leftarrow S_0$ transition and of 13 fs for the $S_2 \leftarrow S_0$ transition at room temperature. From the frequency dependence of the ratio of fluorescence to Raman yields of the $S_1 \leftarrow S_0$ transition we calculate an excited state lifetime of 1.4 ± 0.2 ps using the parameters of the bath derived from the line shape analysis, and irrespective of which master equation is used.

I. INTRODUCTION

In the last decade much progress has been made in the understanding of the optical dynamics of molecules in crystals^{1,2} and glasses.³ Experimentally a variety of techniques are being used to obtain the homogeneous line shape underlying the inhomogeneous absorption spectrum; the most important ones are the photon echo⁴ and spectral hole burning.⁵⁻⁷ Recently these techniques have been extended into the femtosecond time domain enabling study of optical dynamics of molecules in solution.⁸⁻¹⁰ These experiments show that the loss of optical coherence in solution occurs at a time scale of 100 fs, which agrees with the conclusion of earlier degenerate four-wave mixing studies of dye molecules.^{11,12} The finding of such short relaxation times implies that for molecules that exhibit well-resolved vibronic spectra in solution, study of the electronic (vibronic) line shape will directly yield information on the optical dynamics.

Dynamical information can also be obtained from resonance light scattering (RLS) experiments.¹³⁻¹⁶ In the past many such studies have been performed on gaseous¹⁷ and crystalline¹⁸ samples. A few RLS studies have been reported that were aimed at understanding solution dynamics, for example in the study of azulene in CS_2 ¹⁹ and CS_2 in hexane.²⁰ It has been shown^{13,14} that in the so-called fast dephasing limit (*vide infra*) the ratio (R) of the yield of fluorescence and Raman is a direct measure of the system dynamics: $R = 2T_1/T_2^*$, where T_1 is the population relaxation and T_2^* the pure dephasing time constant. This shows that RLS spectroscopy is an attractive alternative to femtosecond transient spectroscopy for obtaining information on the dephasing dynamics, especially in those cases where T_1 is short (< 1 ps).

We have recently started a study of the dephasing dynamics of the lowest optical transitions of azulene in alkanes. Azulene is well-known for its exceptional spectroscopic behavior: it fluoresces efficiently from the second excited singlet state and shows clearly resolved vibrational structure for the two lowest singlet transitions. These characteristics have allowed us to study the dynamics of both origins of azulene

in solution. Furthermore, azulene is a relatively small aromatic molecule, which is an important prerequisite for a molecular dynamics study that is planned to support the development of a microscopic model for the interpretation of these results.

In this paper we report results of a line shape study of the pure electronic $S_1 \leftarrow S_0$ and $S_2 \leftarrow S_0$ transitions of azulene in isopentane and cyclohexane. Two different non-Markovian master equations were used to simulate the line shape of these two optical transitions of azulene in solution. In both master equations the bath correlation function $A(\tau)$ is assumed to show exponential decay. The conclusion from our experiments is that the solution dynamics of azulene falls in the so-called intermediate modulation regime, for which the line shape is neither Gaussian nor Lorentzian. From the line shape analysis it follows that the decay times of the bath correlation function are 25 and 13 fs for the $S_1 \leftarrow S_0$ and the $S_2 \leftarrow S_0$ transitions of azulene, respectively.

We also report on resonance light scattering spectroscopy of the lowest singlet state of azulene in cyclohexane. From the frequency dependence of the ratio between the fluorescence and Raman yields, we calculate a population relaxation time of 1.4 ± 0.2 ps using parameters obtained from the line shape simulation. Our light scattering data, however, are not complete enough to decide upon the question of which master equation should be preferred to describe the optical dynamics in solutions.

II. THEORETICAL CONSIDERATIONS

A. Absorption line shape

In this section we describe the absorption line shape of a molecule in terms of the interaction between a "system," the ground and electronically excited states, and a bath that comprises all other degrees of freedom of the solute and solvent. The line shape function of the absorption spectrum $I(\omega)$ is defined as the Fourier transform of the normalized dipole correlation function²¹:

$$I(\omega) \propto |\mu(0)|^{-2} \int_{-\infty}^{\infty} dt \exp(i\omega t) \langle \langle \mu^H(t) \mu(0) \rangle \rangle, \quad (1)$$

where ω is the photon frequency, $\mu^H(t)$ is the system dipole operator in the Heisenberg representation, and $\langle\langle \ \rangle\rangle$ denotes a trace over the system and the bath. The normalized dipole correlation function can be obtained by solving the *reduced* Liouville equation of motion for the density matrix element $\rho_{21}(t)$, with the initial condition $\rho_{21}(0) = 1$. By making this connection we have used the fact that $\mu_{21}(0)$ is independent of the bath and thus commutes with the trace over the bath degrees of freedom.²²

The line shape function can thus be written in the form:

$$I(\omega) \propto 2 \operatorname{Re} \int_0^\infty dt \exp(i\omega t) \rho_{21}(t). \quad (2)$$

In the fast modulation limit, where $\rho_{21}(t)$ decays exponentially, Eq. (2) predicts a Lorentzian line shape. This description usually works for doped molecular crystals and semiconductors. In solution, however, the bath dynamics may occur on the same time scale as the system dynamics and therefore $\rho_{21}(t)$ depends explicitly on the bath correlation time Λ^{-1} . In this case the relaxation process is non-Markovian.

Two different types of master equations, known as POP and COP,²² have been used to calculate the non-Markovian line shape function. The acronyms POP and COP refer to the way the reduction of the cumulant expansion of the time evolution operator is performed. Mukamel has shown²² that the second-order POP (partial ordering prescription) master equation has the following form:

$$d\rho_{21}/dt = -i\omega_{21}\rho_{21}(t) - \int_0^t d\tau A(t-\tau)\rho_{21}(\tau), \quad (3)$$

where $A(\tau)$ is the bath correlation function.

For the second-order COP (chronological ordering prescription) master equation Mukamel²² has derived the form:

$$d\rho_{21}/dt = -i\omega_{21}\rho_{21}(t) - \int_0^t d\tau A(t-\tau) \exp[-i\omega_{21}(t-\tau)] \rho_{21}(\tau). \quad (4)$$

The difference between these master equations is that by choosing a particular ordering in a truncated cumulant expansion, the statistical properties of the bath are *implicitly* assumed to be different. Mukamel also showed²² that in the fast modulation limit both these equations reduce to the same Markovian equation. In both non-Markovian master equations the bath dynamics have been incorporated in the correlation function $A(\tau)$. If we take for $A(\tau)$ a decaying exponential $A(\tau) = \Delta^2 \exp(-\Lambda\tau)$, Eqs. (3) and (4) lead to the following line shape functions^{22,23}:

$$I^{\text{POP}}(\omega) \propto 2 \operatorname{Re} \int_0^\infty d\tau \exp[i(\omega - \omega_{21})\tau] \exp[-(\Delta^2/\Lambda^2) \times (e^{-\Lambda\tau} - 1 + \Lambda\tau)], \quad (5)$$

$$I^{\text{COP}}(\omega) \propto \Delta^2 \Lambda / [(\omega - \omega_{21} - \Delta)^2 \times (\omega - \omega_{21} + \Delta)^2 + \Lambda^2(\omega - \omega_{21})^2]. \quad (6)$$

In the fast modulation limit, where $\Delta \ll \Lambda$, both line shapes reduce to a Lorentzian with a pure dephasing rate constant $T_2^{*-1} = \Delta^2 \Lambda^{-1}$. The POP line shape Eq. (5) allows for a

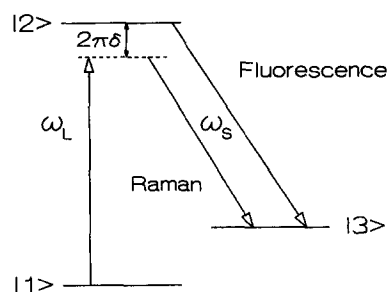


FIG. 1. Molecular energy level diagram and frequencies for resonance light scattering. States $|1\rangle$ and $|3\rangle$ are the ground state and a vibrationally excited state in the S_0 electronic manifold, while $|2\rangle$ is an electronically excited state. Frequencies ω_L and ω_S are the incident and scattered light waves, respectively. The frequency detuning is denoted by δ .

smooth transition from a Gaussian to a Lorentzian line shape, while the COP line shape Eq. (6) corresponds to the two state jump model.^{22,23} The POP master equation takes into account the effects of many perturbing levels and may thus be more suitable for the description of dephasing in the condensed phases.

B. Resonance light scattering spectroscopy

As stated in Sec. I, the resonance light scattering spectrum of a molecule depends on the dephasing dynamics. For a two-level system it has been shown^{13,14} that for the Markovian and low-field limits, the ratio of fluorescence to Rayleigh yields equals $2T_1/T_2^*$. For a three-level Markovian system, depicted in Fig. 1, the same relation is obtained^{16,24} for the relative intensities of the vibrational fluorescence and Raman scattering provided that the different pure dephasing parameters are correlated:

$$\Gamma_{23}^* = \Gamma_{12}^* + \Gamma_{13}^*. \quad (7)$$

Here the pure dephasing parameters Γ_{ij}^* refer to the transitions $i \leftarrow j$ in Fig. 1. The aforementioned results can be derived using the formalism developed by Mollow²⁵ or by using a perturbational approach. In the latter case the use of double-sided Feynman diagrams greatly simplifies the calculation. The relevant diagrams for resonance light scattering in a three-level system are shown in Fig. 2. The rules for working out these diagrams have been given by Yee and

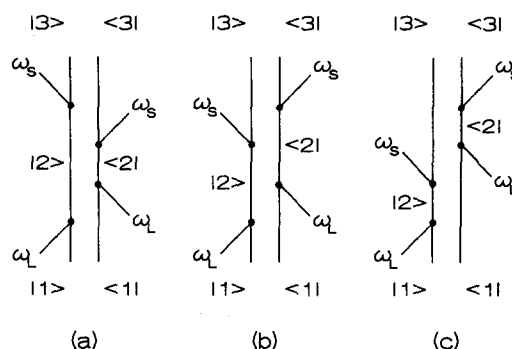


FIG. 2. Double-sided Feynman diagrams for resonance light scattering in a three-level system. Diagrams (a) and (b) contribute only to fluorescence while diagram (c) contributes to both fluorescence and Raman.

Gustafson.²⁶ We note that diagrams (a) and (b) contribute only to fluorescence while diagram (c) contributes to both fluorescence and Raman (Rayleigh for a two-level system). For a two-level system, state $|3\rangle$ should be replaced by $|1\rangle$ in all diagrams and a fourth diagram appears²⁶ that contributes to both fluorescence and Rayleigh scattering.

Using Mollow's formalism²⁵ de Bree and Wiersma calculated^{24,27} the power densities of the vibrational fluorescence and the Stokes-Raman component of the signal in the ultrafast dephasing limit $\Gamma_{12}^* = \Gamma_{23}^* = 1/T_2^*$:

$$I_n(\omega) = F[\chi, T_2, \rho_{11}(\infty)] \times \frac{\Gamma_{23}}{(\omega - \omega_{21} + \omega_{31})^2 + \Gamma_{23}^2} \frac{2T_1 - T_2}{T_2}, \quad (8a)$$

$$I_{\text{Raman}}(\omega) = F[\chi, T_2, \rho_{11}(\infty)] \times \frac{\Gamma_{13}}{(\omega - \omega_L + \omega_{31})^2 + \Gamma_{13}^2}. \quad (8b)$$

Here $F[\chi, T_2, \rho_{11}(\infty)]$ is a measure of the degree of excita-

tion of the system, χ is the Rabi frequency, $\rho_{11}(\infty)$ is the steady-state ground-state population, T_2 is the dephasing time constant at the vibronic transition, and ω_L is the frequency of the laser. From Eqs. (8a) and (8b) we find that the ratio of the integrated fluorescence versus Raman intensities is $2T_1/T_2^*$, thus identical to the result for a two-level system. We recall that this agreement rests upon the assumption that vibrational dephasing is much slower than electronic dephasing. This assumption is clearly warranted for molecules in solution where optical spectra generally are very broad and Raman spectra sharp.

So far we have assumed that our system has Markovian dynamics. This assumption certainly fails for the solution phase. Several attempts have been made to calculate the ratio of fluorescence to Raman yields in the non-Markovian case (R_{nM}). Of course, the result obtained depends on the type of non-Markovian master equation used. When the POP master equation (5) is used for $\rho(t)$, assuming that $A(\tau) = \Delta^2 \exp(-\Lambda\tau)$, R_{nM}^{POP} can be expressed in terms of a continued fraction²⁸:

$$R_{nM}^{\text{POP}} = -2 \operatorname{Im} \left\{ \frac{\Delta^2 T_1}{2\pi\delta + i[\Lambda + 1/(2T_1)] - \frac{2\Delta^2}{2\pi\delta + i[2\Lambda + 1/(2T_1)] - \frac{3\Delta^2}{2\pi\delta + i[3\Lambda + 1/(2T_1)] \dots}} \right\}, \quad (9)$$

where δ is the frequency detuning (in frequency units) from resonance.

Equation (9) shows that R_{nM}^{POP} is dependent on the frequency detuning between the exciting laser and the peak of the absorption, in contrast to the Markovian case, where $R_M = 2T_1/T_2^*$ is independent of frequency detuning. Equation (9) also shows that in the fast modulation (Markovian) limit $\Delta/\Lambda \ll 1$, and in the impact limit $\delta/\Lambda \ll 1$, R_{nM}^{POP} reduces to R_M .

When the COP master equation (6) is used with the same exponential response function for $A(\tau)$, one obtains for R_{nM}^{COP} :^{27,29,30}

$$R_{nM}^{\text{COP}} = \frac{2T_1\Delta^2\Lambda^{-1}}{1 + (2\pi\delta)^2\Lambda^{-2}}. \quad (10)$$

Again R_{nM}^{COP} is frequency dependent through the parameter δ in Eq. (10). In the Markovian limit $\Delta/\Lambda \ll 1$ and under the condition that $\delta/\Lambda \ll 1$, R_{nM}^{COP} also reduces to R_M .

III. EXPERIMENTAL SECTION

Azulene (Janssen) was purified once by sublimation. The solvents cyclohexane (Merck, p.a.) and isopentane (Fluka, p.a.) were distilled before use. The samples used for the absorption experiments contained 10^{-3} M azulene. The low temperature absorption spectra were taken using a Cary 210 spectrophotometer equipped with a small cryostat. A Perkin Elmer Lambda 5 spectrophotometer was used for measurement of the high temperature absorption spectra. All spectra were digitized afterwards. Because of vibrational congestion the fits to the absorption line shape were made on

the red flank of the origin transitions. In the case of the $S_1 \leftarrow S_0$ transition a hot band at 821 cm^{-1} was included in the fit procedure, assuming the same line broadening mechanism as for the origin.

The resonance Raman spectra were taken using a pyridine-1 dye laser pumped by an argon ion laser. Wavelengths between 690 and 720 nm at average power levels between 50 and 150 mW were used to excite the sample (0.03 M azulene in cyclohexane at 295 K placed in a magnetically stirred quartz cell). A right angle scattering geometry was used and the scattered light was passed through a Spex 1402 double monochromator equipped with two 1800 gr/mm gratings. The slit width was set such that the effective resolution was 10.5 cm^{-1} at 632 nm. The resonance light scattering signal was measured using a cooled RCA C31034 phototube with an Ortec 770 photon counter. The ratio of the fluorescence versus Raman yields as a function of detuning was calculated by integrating both components in the emission spectrum between 725 to 860 nm (550 to 2770 cm^{-1} from the origin). In the analysis of the data it was assumed that this ratio is identical to the ratio obtained by measurement of the complete emission spectrum, after correction for the instrumental response.

IV. RESULTS AND DISCUSSION

Figures 3(a) and 3(b) show the room temperature absorption spectra of azulene in isopentane. The absorption spectra of azulene in cyclohexane were found to be indistinguishable. The origins of both singlet transitions are indicated by an asterisk and observed at 697.5 nm ($S_1 \leftarrow S_0$) and

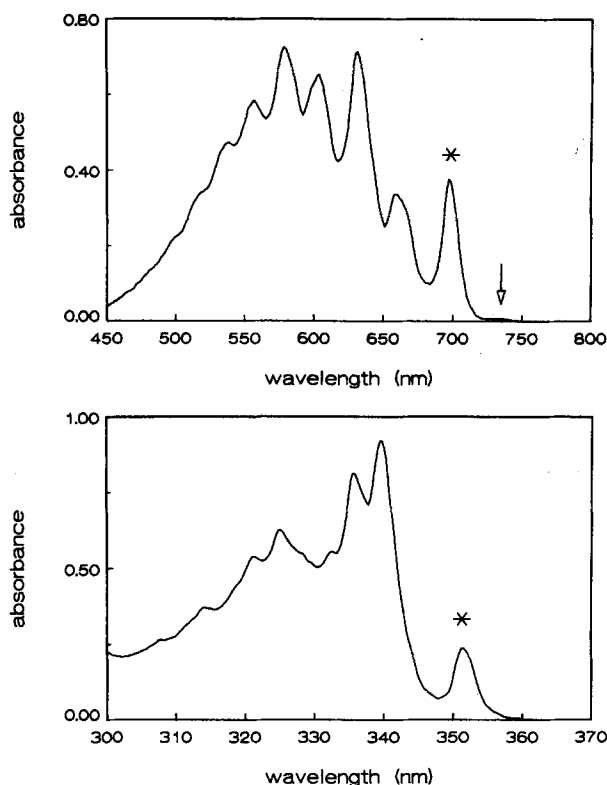


FIG. 3. Room temperature absorption spectra of azulene in isopentane. (a) Shows the $S_1 \leftarrow S_0$ vibronic manifold and (b) the $S_2 \leftarrow S_0$ vibronic manifold. The origin of each transition is indicated by an asterisk; the arrow marks a hot-band.

352.2 nm ($S_2 \leftarrow S_0$). In the spectrum of the $S_1 \leftarrow S_0$ transition a hot-band, marked by an arrow, is observed at 821 cm^{-1} on the red side of the origin. Figure 3 also shows that both origin transitions are clearly spectrally resolved. This enabled us to make a reliable analysis of the line shape of these transitions. Figures 4(a) and 4(b) show an enlarged view of both origin transitions at room temperature and fits to the POP line shape given in Eq. (5). From this fit a bath correlation time (Λ^{-1}) of 25 fs for S_1 and 13 fs for S_2 is obtained. These short bath correlation times are probably due to torsional and angular motions of the isopentane molecules colliding with the azulene molecule. Molecular dynamics simulations need to be performed to check this idea. When the COP line shape, given in Eq. (6), is used for the simulation, the corresponding bath correlation times are found to be 13 and 8 fs for S_1 and S_2 , respectively. The line shape simulations also yield values for the amplitude (Δ) of the stochastically fluctuating force. These are found to be much less dependent on whether the COP or the POP line shape is used. The insert in Figs. 4(a) and 4(b) shows the difference between the simulated line profiles and the experimentally observed ones. The oscillatory pattern found for this difference for both transitions questions the assumption of exponential decay of the bath correlation function. Further studies regarding this point will be made.

Sue *et al.*³¹ and Mukamel³² analyzed Raman excitation profiles of the lowest singlet transition of azulene in CS_2 ¹⁹ with the aim of obtaining dynamical information. They used the POP master equation in their analysis and obtained a

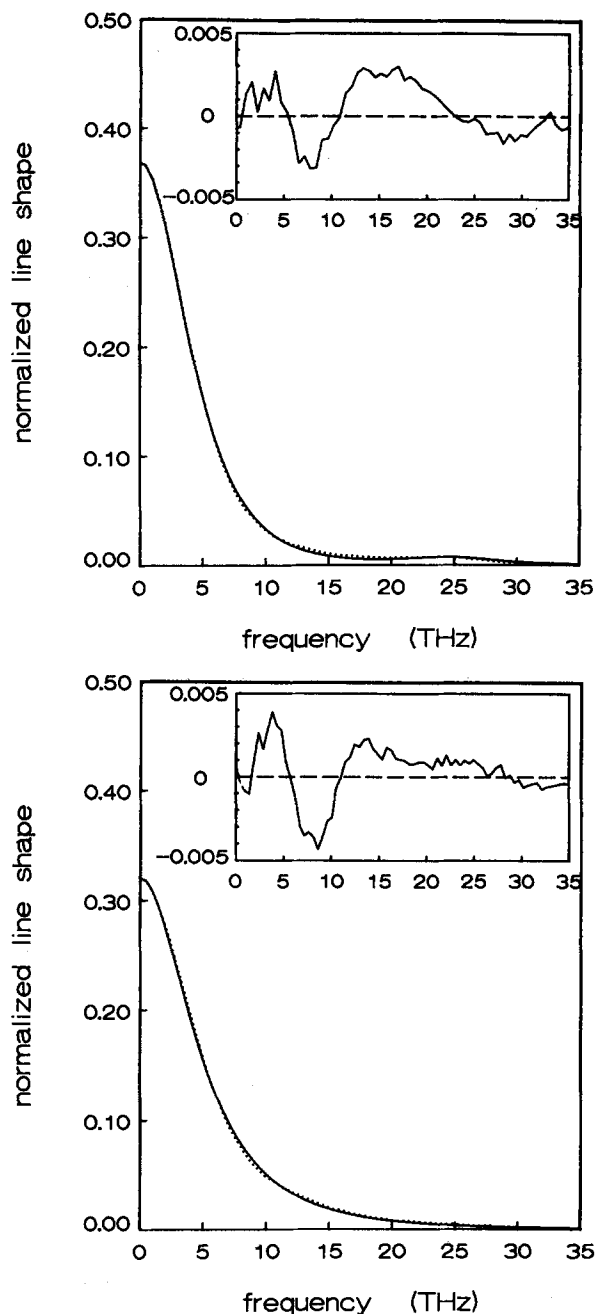


FIG. 4. Line shapes of the origins of (a) the $S_1 \leftarrow S_0$ and (b) the $S_2 \leftarrow S_0$ electronic transitions of azulene in isopentane at room temperature. The experimental results (dotted curves) are shown together with the simulated curves (solid lines), based on the POP line shape [Eq. (5)]. The relevant parameters are (a) $\Delta = 35 \text{ THz}$, $\Lambda = 36 \text{ THz}$ for S_1 and (b) $\Delta = 53 \text{ THz}$, $\Lambda = 85 \text{ THz}$ for S_2 . The difference between the calculated and experimentally measured line shape is given in the insert.

bath correlation time of about 300 fs. Our line shape analysis of the $S_1 \leftarrow S_0$ transition of azulene in CS_2 yields a bath correlation time of 30 fs, which is close to what we found for azulene in isopentane. For Δ we obtain a value of about 45 THz. In the notation of Sue *et al.*,³¹ we find that $\kappa = \Lambda/\Delta \approx 0.7$ instead of 0.1.^{31,32}

We obtain for the POP and COP line shape simulations of azulene in alkanes about the same variance between calculated and measured line shape function. This means that on the basis of only a line shape analysis a sensible choice

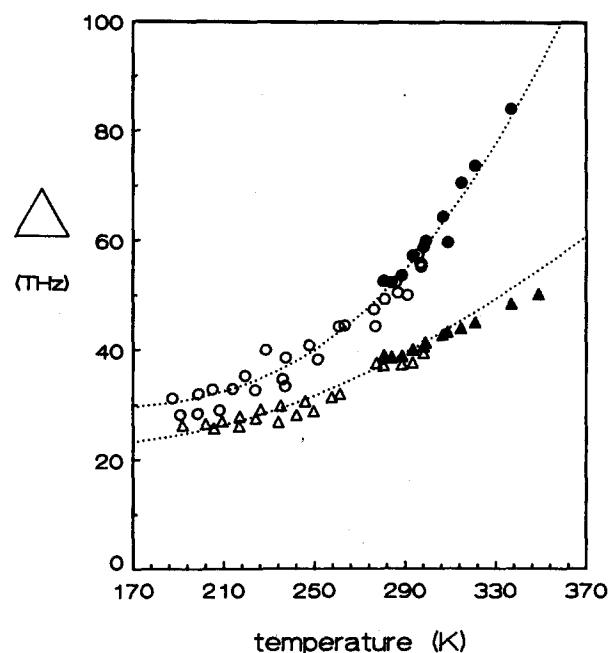
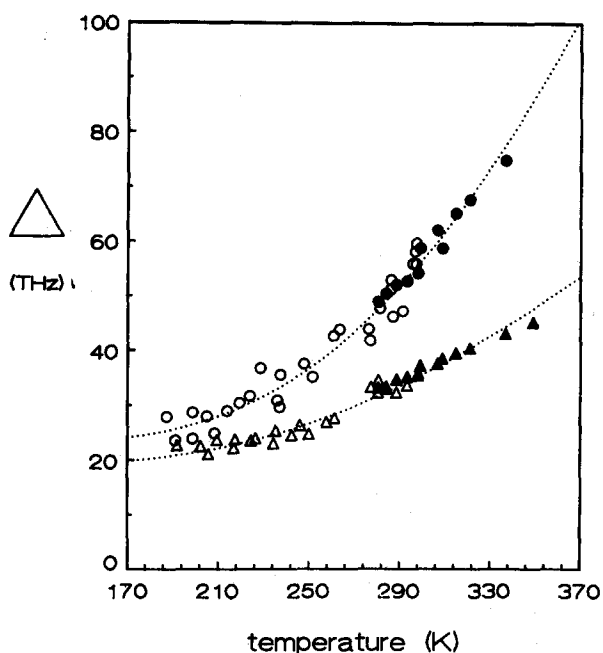
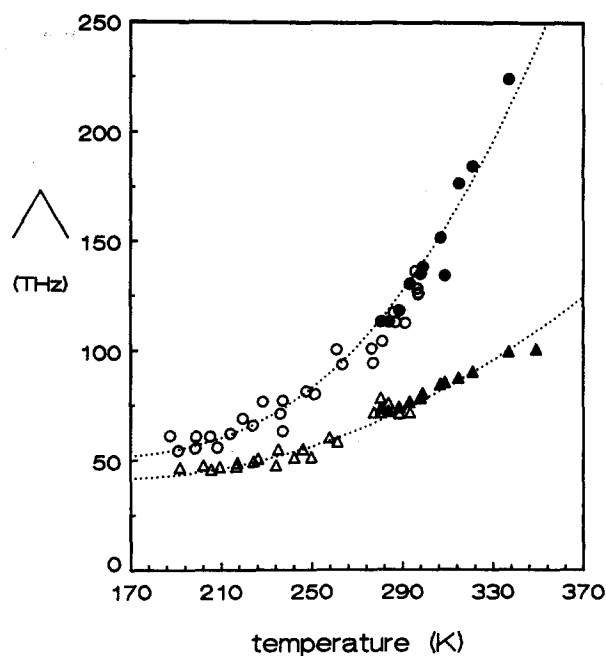
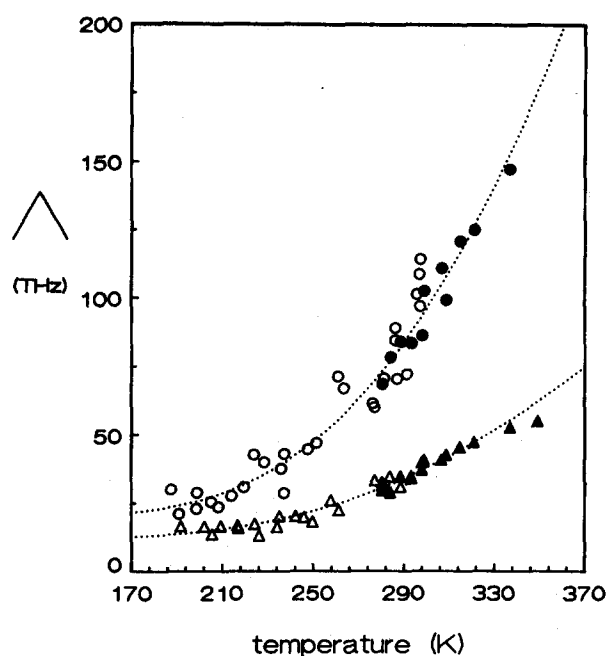


FIG. 5. Temperature dependence of (a) the inverse correlation time Λ , and (b) the variance Δ according to the POP line shape function [Eq. (5)]. The $S_1 \leftarrow S_0$ (triangles) and $S_2 \leftarrow S_0$ (circles) transitions of azulene were studied in isopentane (open symbols) and cyclohexane (filled symbols). The dotted lines are of the form of Eq. (11), with constants given in Table I.

FIG. 6. Temperature dependence of (a) the inverse correlation time Λ , and (b) the variance Δ according to the COP line shape function [Eq. (6)]. The symbols are as in Fig. 5 and the appropriate constants used in the simulations are given in Table I.

between the POP and COP models is impossible. However, when the line shape is fitted to a Voigt profile the variance is a factor of 10–100 higher. This indicates that a separation between slow and fast fluctuations in the bath is not warranted. Hence a non-Markovian master equation approach to the line shape is necessary. Figures 5 and 6 present the results of such an analysis for both azulene transitions over a wide temperature range using isopentane (open symbols) and cyclohexane (filled symbols) as solvents. These figures show that the dynamics of the two azulene transitions are rather different, but that the same trend is found for the tempera-

ture dependence of the Δ 's and Λ 's, irrespective of whether the POP or COP line shape is used. However, the absolute value of the bath correlation time is dependent on the model used. When the POP master equation is used the derived bath correlation time is about a factor of two longer than with the COP master equation.

Finally, we observe that with rising temperature the lowest singlet transition exhibits a red shift of about 50 cm^{-1} , while the second singlet transition in azulene remains stationary under the same conditions.

For both transitions we find that $\Delta\Lambda^{-1} \approx 1$, irrespective of the model used, which implies that the azulene dynamics

in isopentane (and cyclohexane) fall into the so-called intermediate modulation regime. For cresyl violet in ethylene glycol it was concluded from an analysis¹⁰ of femtosecond hole burning experiments⁸ that $\Delta\Lambda^{-1} \gg 1$. The bath correlation time was calculated to be about 150 fs, which is about a factor of 10 longer than for azulene in cyclohexane. A possible reason for the different behavior of the molecular dynamics is that in ethylene glycol the hydrogen bonding and the high viscosity prevent fast changes in the coordination of a solute molecule. In hydrocarbon solutions, fast diffusion or reorientation of molecules in the first shell around the caged molecule may occur, which leads to fast fluctuations in the bath.

Leaving aside for the moment the question of which master equation describes best the azulene dynamics, we discuss the trend observed in the data presented in Figs. 5 and 6. These figures show that at the lowest temperatures of our measurements the bath parameters for both S_2 and S_1 are almost the same. For temperatures higher than 200 K the dynamics for the two states begin to differ with the line shape of the $S_2 \leftarrow S_0$ transition being much more temperature dependent than that of the $S_1 \leftarrow S_0$ transition. Figures 5 and 6 further show that the molecular dynamics vary continuously on switching from isopentane to cyclohexane as a solvent. As currently no theory exists to simulate the temperature dependence of the bath parameters, we have attempted to fit them using an Arrhenius-type equation:

$$B(T) = B_0 + B_1 \exp(-\Delta E/kT), \quad (11)$$

where B is Δ or Λ for S_1 or for S_2 . The activation energy obtained from a fit of the data to Eq. (11) for both S_1 and S_2 is about 800 cm^{-1} . The dotted lines in Figs. 5 and 6 present fits to Eq. (11) with parameters given in Table I. Since the 800 cm^{-1} activation energy corresponds to a typical molecular vibrational frequency, this analysis suggests that vibrations play an important role in the dephasing process. The different dynamical behavior of the two azulene transitions must then be assigned to a difference in the vibrational force field of the two electronic states. Our data suggest that the frequencies of the thermally accessible vibrations in the S_1 state are closer to the ground state values than those for the S_2 state. What is known about the low-frequency vibrations of azulene from experiments^{18,33} supports this idea. From the fact that the $S_1 \leftarrow S_0$ line shape is much less dependent on

temperature than the line shape for the $S_2 \leftarrow S_0$ transition and the fact that the $S_1 \leftarrow S_0$ transition undergoes a substantial red shift with rising temperature, we suggest that coherence exchange^{34,35} may contribute to the dephasing dynamics of the lowest singlet transition. For the $S_2 \leftarrow S_0$ transition, uncorrelated vibrational scattering is presumably the dominant dephasing mechanism and in this case no temperature dependent frequency shift is expected.^{34,35} For this relaxation model, in which many vibrational modes play an essential role in the dephasing dynamics, we expect the POP master equation to be more suitable than the COP for the description of the dynamics.

One might wonder whether the difference in dynamical behavior of the two transitions could be caused by direct coupling between the transition dipole of azulene and the solvent molecules. In such a model the induced dipoles in the solvent molecules would produce a fluctuating field by rotational and translational motion that would interrupt the phase of the molecular oscillator. The dynamics in this model would be directly related to the magnitude of the transition dipole and to the viscosity of the solvent. In the case of azulene we found, as shown in Figs. 5 and 6, that changing the solvent from isopentane to cyclohexane makes no difference in the optical dynamics, despite the fact that the viscosity of isopentane is more than a factor of 3 lower than that of cyclohexane.³⁶ To assess the effect of the magnitude of the transition dipole on the dynamics, we studied the line shape of anthracene in the same solvents. We found that the temperature dependence of the line shape of anthracene better resembles that of the lower (weakest) azulene transition than the higher one that has a transition dipole comparable to anthracene. This shows that the magnitude of the transition dipole itself is not an important factor in determining the dynamics.

We now present and discuss the results obtained from a resonance light scattering study of azulene. As this technique is only practical for the investigation of short-lived excited states (see Sec. II B) we can only use it for a study of the lowest singlet state of azulene. Figure 7 shows the room temperature resonance (zero-frequency detuning) light scattering spectrum of the $S_1 \leftarrow S_0$ transition of azulene in

TABLE I. Parameters for the Arrhenius-type activation of the inverse correlation time Λ and the variance Δ in the POP and COP approximations. The results for both the $S_1 \leftarrow S_0$ and the $S_2 \leftarrow S_0$ electronic transitions of azulene are given in THz.

	(a) POP		(b) COP	
	$S_1 \leftarrow S_0$	$S_2 \leftarrow S_0$	$S_1 \leftarrow S_0$	$S_2 \leftarrow S_0$
Λ	$B_0 = 12$ $B_1 = 2900$ $\Delta E = 29$	$B_0 = 20$ $B_1 = 10\,000$ $\Delta E = 30$	$B_0 = 40$ $B_1 = 2600$ $\Delta E = 26$	$B_0 = 50$ $B_1 = 15\,000$ $\Delta E = 31$
Δ	$B_0 = 19$ $B_1 = 800$ $\Delta E = 24$	$B_0 = 23$ $B_1 = 2900$ $\Delta E = 24$	$B_0 = 22$ $B_1 = 700$ $\Delta E = 24$	$B_0 = 29$ $B_1 = 5000$ $\Delta E = 30$

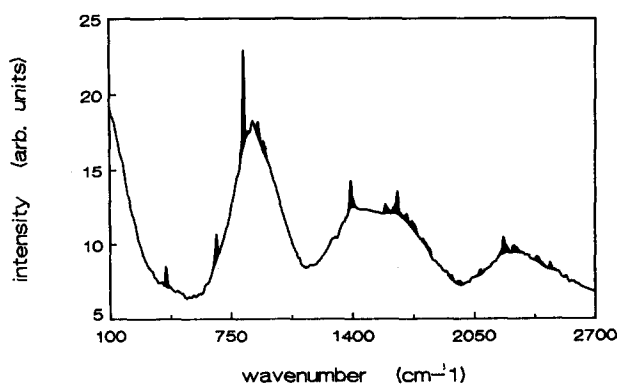


FIG. 7. Room temperature resonance light scattering spectrum for the $S_1 \leftarrow S_0$ electronic transition of azulene in cyclohexane. The sharp Raman features (dark) are clearly distinct from the broad underlying fluorescence bands. Solvent Raman signals were subtracted.

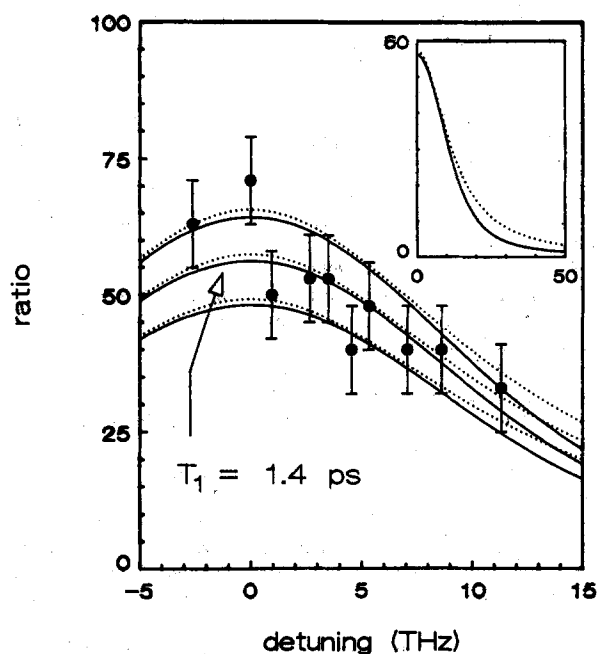


FIG. 8. Ratio R of the fluorescence to Raman yields (filled circles) as a function of frequency detuning of the excitation laser. The predicted functional dependence of this ratio is shown using the POP (solid lines) and the COP (dotted lines) master equation for three values of the lifetime T_1 ranging from 1.6 ps (above) to 1.2 ps (below). The insert shows that at larger frequency detunings a distinction between the models can be made.

cyclohexane. The sharp features constitute the Raman spectrum and the broad features the dephasing-induced fluorescence spectrum of azulene. The frequencies of the Raman active vibrations observed in the spectrum correspond with those reported by other workers.^{18,37,38} Figure 8 shows the ratio of fluorescence to Raman yields as a function of frequency detuning and the predicted functional dependence of this quantity for both the COP and POP model with different population relaxation times. In these fits we used the bath parameters Δ and Λ obtained from the absorption line shape analyses. It is clear from Fig. 8 that both the COP and POP models yield fits that are consistent with the data over this limited range of frequency detuning. The insert of Fig. 8 shows that for larger detunings a clear distinction between the different models can be made. Unfortunately, with our current detection sensitivity we cannot perform measurements for larger frequency detunings than shown in Fig. 8. Also, for larger detunings, the assumption of a three level system for the scattering process becomes questionable because more vibronic transitions will contribute to the polarizability.

The fits to the data in Fig. 8 allow us also to deduce that the lifetime of the lowest singlet state in azulene in cyclohexane is 1.4 ± 0.2 ps, using either the COP or the POP model. This deduced lifetime is close to the previously reported lifetime of 1.9 ± 0.2 ps for azulene in cyclohexane by Ippen³⁹ and Shank *et al.*⁴⁰ From the fact that the lifetime calculated from the light scattering data agrees with the measured lifetime we conclude that the line shape analysis is a useful means of calculating the bath parameters.

Finally we note that the results presented in Fig. 8 are

not consistent with a bath correlation time of about 300 fs as deduced by Sue *et al.* for azulene in CS_2 .³¹ These authors already noted that quantum yield measurements of Raman versus fluorescence are a more sensitive probe to the ratio of the bath parameters than Raman excitation profiles. We therefore conclude that for the azulene in CS_2 the bath correlation time is about 30 instead of 300 fs.

V. SUMMARY AND CONCLUSIONS

We conclude from an absorption line shape analysis and resonance light scattering study of azulene in hydrocarbon solutions that a non-Markovian master equation is needed to describe the optical dynamics for the two lowest singlet excitations. Using a stochastic model for the bath dynamics, the dephasing is shown to occur in the so-called intermediate modulation regime: $\Delta\Lambda^{-1} \approx 1$, where Δ is the amplitude and Λ is the correlation time of the stochastically fluctuating force.

All results are consistent with bath correlation times of about 20 fs, but the available data do not allow to distinguish between the POP and COP non-Markovian master equations. Süsse *et al.*⁴¹ recently showed that photon echoes in solution can only be observed for delay times much shorter than the bath correlation time. It seems then that for the azulene system, femtosecond hole burning⁸ is a more suitable technique than the photon echo to study the bath dynamics directly.

We further suggest that the different dynamic behavior of the first and second singlet state in azulene is because of a difference in vibrational force field. Dephasing is a result of the fact that fluctuations in the bath sweep the optical oscillator to various hot bands that are off-resonant with the origin transition. For the lowest singlet transition of azulene we suggest that coherence exchange plays a role in the relaxation dynamics.

Note added in proof: Using the technique of time-resolved two-photon absorption spectroscopy³⁹ at the origin transition we have recently determined the excited state lifetime of azulene in cyclohexane at room temperature to be 1.6 ± 0.2 ps. This lifetime is somewhat shorter than reported in Refs. 39 and 40 for excitation into the vibronic manifold and is in excellent agreement with the excited state lifetime of 1.4 ± 0.2 ps derived from the resonance light scattering spectra of azulene discussed in Sec. IV.

A detailed account of this work will be published elsewhere.

ACKNOWLEDGMENTS

We thank Dr. H. W. den Hartog for loan of the dye laser, and F. de Haan for the instrument control and data analysis programs. We are indebted to Professor S. Mukamel of the University of Rochester for enlightening correspondence on the connection between the dipole correlation function and the reduced density matrix. We also gratefully acknowledge Dr. E. W. Castner for useful comments and perusal of the manuscript. The investigations were supported by the Netherlands Foundation for Chemical Research (SON) with financial aid from the Netherlands Organization for the Advancement of Science (NWO).

- ¹ C. A. Walsh, M. Berg, L. R. Narasimhan, and M. D. Fayer, *Acc. Chem. Res.* **20**, 120 (1987).
- ² D. A. Wiersma and K. Duppen, *Science* **237**, 1147 (1987).
- ³ R. Jankowiak and G. J. Small, *Science* **237**, 618 (1987).
- ⁴ (a) N. A. Kurnit, I. D. Abella, and S. R. Hartmann, *Phys. Rev. Lett.* **13**, 567 (1964); (b) I. D. Abella, N. A. Kurnit, and S. R. Hartmann, *Phys. Rev.* **141**, 391 (1966).
- ⁵ B. M. Kharlamov, R. I. Personov, and L. A. Bykovskaya, *Opt. Commun.* **12**, 191 (1974).
- ⁶ A. A. Gorokhovskii, R. K. Kaarli, and L. A. Rebane, *JETP Lett.* **20**, 216 (1974).
- ⁷ H. de Vries and D. A. Wiersma, *Phys. Rev. Lett.* **36**, 91 (1976).
- ⁸ C. H. Brito Cruz, R. L. Fork, W. H. Knox, and C. V. Shank, *Chem. Phys. Lett.* **132**, 341 (1986).
- ⁹ P. C. Becker, H. L. Fragnito, J. Y. Bigot, C. H. Brito Cruz, R. L. Fork, and C. V. Shank, *Phys. Rev. Lett.* **63**, 505 (1989).
- ¹⁰ W. Vogel, D.-G. Welsch, and B. Wilhelm, *Chem. Phys. Lett.* **153**, 376 (1988); *Phys. Rev. A* **37**, 3825 (1988).
- ¹¹ T. Yajima and H. Souma, *Phys. Rev. A* **17**, 309 (1978).
- ¹² H. Souma, E. J. Heilweil, and R. M. Hochstrasser, *J. Chem. Phys.* **76**, 5693 (1982).
- ¹³ V. Hizhnyakov and I. Tehver, *Phys. Status Solidi* **21**, 755 (1967); **39**, 67 (1970); **95**, 65 (1979); *Opt. Commun.* **32**, 419 (1980).
- ¹⁴ D. L. Huber, *Phys. Rev.* **158**, 843 (1967); **170**, 418 (1968); **178**, 93 (1969); **187**, 392 (1969); *Phys. Rev. B* **1**, 3409 (1970).
- ¹⁵ Y. R. Shen, *Phys. Rev. B* **9**, 622 (1974).
- ¹⁶ F. A. Novak, J. M. Friedman, and R. M. Hochstrasser, in *Laser and Coherence Spectroscopy*, edited by J. I. Steinfeld (Plenum, New York, 1978), p. 451.
- ¹⁷ J. L. Carsten, A. Szöke, and M. G. Raymer, *Phys. Rev. A* **15**, 1029 (1977).
- ¹⁸ R. M. Hochstrasser and C. A. Nyi, *J. Chem. Phys.* **70**, 1112 (1979).
- ¹⁹ O. Brafman, C. K. Chan, B. Khodadoost, J. B. Page, and C. T. Walker, *J. Chem. Phys.* **80**, 5406 (1984); C. K. Chan, J. B. Page, D. L. Tonks, O. Brafman, B. Khodadoost, and C. T. Walker, *ibid.* **82**, 4813 (1985).
- ²⁰ A. B. Myers, B. Li, and X. Ci, *J. Chem. Phys.* **89**, 1876 (1988).
- ²¹ B. J. Berne and G. D. Harp, *Adv. Chem. Phys.* **17**, 63 (1970).
- ²² S. Mukamel, *Chem. Phys.* **37**, 33 (1979).
- ²³ R. Kubo, in *Fluctuation, Relaxation and Resonance in Magnetic Systems*, edited by D. Ter Haar (Oliver and Boyd, Edinburgh, 1962), p. 23; *Adv. Chem. Phys.* **15**, 101 (1969).
- ²⁴ P. de Bree and D. A. Wiersma, in *Proceedings of the VIIth International Conference on Raman Spectroscopy*, edited by W. F. Murphy (North Holland, New York, 1980), p. 462.
- ²⁵ B. R. Mollow, *Phys. Rev.* **188**, 1969 (1969).
- ²⁶ T. K. Yee and T. K. Gustafson, *Phys. Rev. A* **18**, 1597 (1978).
- ²⁷ P. de Bree, thesis, University of Groningen, The Netherlands, 1981.
- ²⁸ Y. J. Yan and S. Mukamel, *J. Chem. Phys.* **86**, 6085 (1987).
- ²⁹ A. Ron and A. Ron, *Chem. Phys. Lett.* **58**, 329 (1978).
- ³⁰ S. Mukamel, *J. Chem. Phys.* **71**, 2884 (1979).
- ³¹ J. Sue, Y. J. Yan, and S. Mukamel, *J. Chem. Phys.* **85**, 462 (1986).
- ³² S. Mukamel, *Adv. Chem. Phys.* **70**, 165 (1988).
- ³³ M. Fujii, T. Ebata, N. Mikami, and M. Ito, *Chem. Phys.* **77**, 191 (1983).
- ³⁴ P. de Bree and D. A. Wiersma, *J. Chem. Phys.* **70**, 790 (1979).
- ³⁵ Y. Ohtsuki and Y. Fujimura, *J. Chem. Phys.* **91**, 3903 (1989).
- ³⁶ F. D. Rossini, K. S. Pitzer, R. L. Arnett, R. M. Braun, and G. C. Pimentel, in *Selected Values of Physical and Thermodynamic Properties of Hydrocarbons and Related Compounds* (Carnegie, Pittsburgh, PA, 1953), p. 232.
- ³⁷ R. S. Chao and R. K. Khanna, *Spectrochim. Acta A* **33**, 53 (1977).
- ³⁸ J. R. Cable and A. C. Albrecht, *J. Chem. Phys.* **84**, 1969 (1986).
- ³⁹ E. P. Ippen, C. V. Shank, and R. L. Woerner, *Chem. Phys. Lett.* **46**, 20 (1977).
- ⁴⁰ C. V. Shank, E. P. Ippen, O. Teschke, and R. L. Fork, *Chem. Phys. Lett.* **57**, 433 (1978).
- ⁴¹ K.-E. Süsse, W. Vogel, and D.-G. Welsch, *Chem. Phys. Lett.* **162**, 287 (1989).